AGU ADVANCING EARTH AND SPACE SCIENCES

Water Resources Research

RESEARCH ARTICLE
10.1029/2025WR041260

Numerical Analysis of Local Thermal Non-Equilibrium Experiments Reveals Conceptual Regimes of Grain-Scale Heat Transport

Haegyeong Lee[1], Hannah Gebhardt[2], Philipp Blum[1], Peter Bayer[2], and Gabriel C. Rau[3]

[1]Institute of Applied Geosciences (AGW), Karlsruhe Institute of Technology (KIT), Karlsruhe, Germany, [2]Department of Applied Geology, Martin Luther University Halle-Wittenberg, Halle, Germany, [3]School of Environmental and Life Sciences, The University of Newcastle, Callaghan, NSW, Australia

Key Points:

- Analysis of experimental local thermal non-equilibrium (LTNE) effects considering heat transfer across phases using a 2D numerical model
- Anomalous experimental observations are attributed to the strong influence of non-uniform flow and obscure LTNE effects
- LTNE by heat transfer across phases is negligible, but LTNE due to the presence of two phases warrants consideration at the granular scale

Correspondence to:
H. Lee,
haegyeong.lee@kit.edu

Citation:
Lee, H., Gebhardt, H., Blum, P., Bayer, P., & Rau, G. C. (2025). Numerical analysis of local thermal non-equilibrium experiments reveals conceptual regimes of grain-scale heat transport. *Water Resources Research*, *61*, e2025WR041260. https://doi.org/10.1029/2025WR041260

Received 6 JUN 2025
Accepted 17 OCT 2025

Author Contributions:
Conceptualization: Haegyeong Lee, Peter Bayer, Gabriel C. Rau
Formal analysis: Haegyeong Lee
Funding acquisition: Peter Bayer, Gabriel C. Rau
Methodology: Haegyeong Lee
Software: Haegyeong Lee
Supervision: Gabriel C. Rau
Validation: Haegyeong Lee
Writing – original draft: Haegyeong Lee
Writing – review & editing: Hannah Gebhardt, Philipp Blum, Peter Bayer, Gabriel C. Rau

Abstract Modeling heat transport in saturated porous media typically assumes local thermal equilibrium (LTE) conditions, though this assumption lacks justification. Recent work has revealed local thermal non-equilibrium (LTNE) effects for groundwater flow conditions, which standard one-dimensional analytical and numerical models fail to capture accurately. In this study, we develop and validate a 2D numerical model for two-phase heat transport at the granular scale to describe experimental LTNE effects previously observed, by coupling heat fluxes in both phases with a heat transfer term. Our results show that LTNE and non-uniform flow effects are superimposed and challenging to disentangle. However, the experimental results, expressed as temperature difference between solid and fluid phase ($\Delta T(t)$), best match the case where the heat transfer coefficient $h_{sf} \rightarrow \infty$ (maximal efficiency), showing that h_{sf} is insensitive for flow rates of 3–23 m d^{-1} and grain sizes of 5–30 mm. The model further confirms that different and negative $\Delta T(t)$ for same grain sizes are caused by non-uniform flow where arrival of the thermal front varies at the grain scale. Overall, our findings reveal multiple different heat transport concepts: (a) LTE, which is widely used; (b) Baseline LTNE, arises from different thermal properties between phases; (c) Phase transfer LTNE, which involves a limited heat transfer rate between phases; (d) Non-uniform flow LTNE, which is caused by pore-scale flow variations. This detailed concept of LTNE effects suggests that interphase heat transfer plays a negligible role toward LTNE effects at the granular scale under conditions relevant for hydrogeology.

Plain Language Summary Heat transport in porous aquifers, as natural porous media, is commonly modeled with the simplification that the fluid phase like water and the solid phase like grains have always the same temperature, termed "local thermal equilibrium (LTE)," while the detailed approach "local thermal non-equilibrium (LTNE)" allows temperature difference between the phases. This study investigates LTNE effects based on experimental data in the literature using a 2D numerical model to understand the phenomena at the granular scale and provide fundamental findings relevant to natural systems. The model enables to distinguish the heat transfer process between the two phases in LTNE effects from other thermal processes. In the model, non-uniform flow observed in the literature is integrated, showing its influence of preferential flow pathways on LTNE. Based on the results, we identify four conceptual LTNE regimes, categorizing the controlling factors to guide the future research on multi-scale LTNE processes.

1. Introduction

Heat transport modeling for saturated porous media has dragged attention to resolve various scientific and engineering problems, for example, prediction of heat propagation induced by geothermal systems with high accuracy (e.g., Anibas et al., 2018; Di Dato et al., 2022; Hamidi et al., 2019), determination of aquifer properties by heat tracer (e.g., Rau et al., 2014), and optimization of pebble-bed reactor design (e.g., Zhu et al., 2019). Especially for geothermal systems, heat transport models can provide the fundamental information for efficient system performance and spatial arrangement avoiding thermal interference between systems (Pophillat et al., 2020). The accurate prediction of heat transport profits various applications in science and engineering fields.

In the presence of fluid flow in porous media, heat transport can be described by the advection-diffusion equation. Heat transport can be modeled by two different approaches. One approach describes heat transport with an instant thermal equilibrium between fluid and solid phases in porous media, which is termed local thermal equilibrium

(LTE) model, while the other approach considers local temperature difference between two phases, which is termed local thermal non-equilibrium (LTNE) model. Yet, the definition of LTNE remains unspecified in the literature due to the lack of a detailed mechanism. The most detailed definition by Kaviany (1995) describes LTNE as thermal disequilibrium between fluid and solid phases in a two-medium treatment of porous media. They consider that two phases are coupled through a heat transfer term, which can either be approached by examination of the microstructure or by empiricism. Nield and Bejan (2017) define LTNE as a condition in which LTE is absent, allowing heat transfer between fluid and solid phases. They claimed that the determination of an appropriate heat transfer term is crucial for the application of this model. Heinze (2024) stated that LTNE assumption considering a difference of temperature between the involved phases could improve interpretation of natural systems. These studies postulate that accurate prediction of heat transport requires appropriate estimation of the heat transfer coefficient in LTNE models, which describes heat transfer between phases.

Theoretical considerations and experiments by Levec and Carbonell (1985a, 1985b) illustrated that LTNE effects should show up as a delayed temperature response of the solid phase compared to the fluid phase in response to a temperature transient. According to their definition, LTNE effects can be detected experimentally by determining the temperature difference between the fluid and solid phases. Bandai et al. (2023) followed the same approach to measure the temperature of the fluid and solid phases separately. Through the method, they detected temperature difference between two phases as evidence of LTNE effects for a single grain size. They illustrated that larger Darcy velocities and smaller effective thermal conductivity of the fluid can increase the magnitude of the temperature difference between two phases. Lee et al. (2025) also conducted heat transport experiments by measuring fluid and solid temperature separately, demonstrating the enhancement of LTNE effects by increasing flow velocities and grain sizes. Notably, they demonstrated the evidence of non-uniform flow effects in homogeneous porous media. This is also shown by the study of Rau et al. (2012) with heat transport experiments in homogeneous sand. They reported significant non-uniform flow for increasing flow velocity. Since LTNE experiments are based on measuring the temperature difference between solid and fluid at the granular scale, the influence of non-uniform flow makes the quantitative analysis of LTNE challenging.

LTNE can also be inferred experimentally without measurement of the temperature difference between fluid and solid phases by comparing the velocities derived from solute and thermal experiments in the same media (Baek et al., 2022; Gossler et al., 2019). This requires a comparison of an effective and an apparent retardation factor. The effective retardation factor is determined using the solute velocity (which corresponds to the seepage velocity) and the thermal front velocity. The apparent thermal retardation is derived from a comparison between volumetric heat capacities of the porous media and the fluid phase. LTNE conditions exist when effective and apparent retardation factors are unequal (Gossler et al., 2019). However, this approach only offers indirect evidence of LTNE effects.

LTNE effects can be modeled with different numerical solutions (Bandai et al., 2023; Gossler et al., 2020; Roshan et al., 2014; Shi et al., 2024; Wang & Fox, 2022). Although an analytical solution for the two equation model is available, it is limited to situations where specific assumptions (i.e., fluid in dispersed plug flow, axial heat conduction in the solid phase) apply (Wakao & Kaguei, 1982). Therefore, LTNE effects are usually modeled numerically to simulate heat transport under groundwater flow conditions. The modeled LTNE effects can be validated with experimental data. We note that Levec and Carbonell (1985a) and Bandai et al. (2023) analyzed their data by their models without spatially distinguishing fluid and solid phases. Further, their one-dimensional (1D) simulations only allow to distinguish temperature in the flow direction, whereas the temperature in the transverse direction is assumed to be locally equilibrated. While Wang and Fox (2023) developed a 1D model that separates fluid and solid phases, their approach remains limited to ideal uniform flow conditions. This simplification is unrealistic for describing heat transport in natural environments and reveals the necessity to consider more spatial dimensions when assessing LTNE effects.

Different and partly contradictory criteria for LTNE effects under the unconsolidated porous aquifer conditions have been proposed by previous studies. The numerical modeling results by Gossler et al. (2020) show that LTNE does not occur for small Darcy velocities (<1.6 m d^{-1}) and small grain sizes (<7 mm), which cover from conduction dominant to transition regime. Experiments conducted by Baek et al. (2022) reveal that LTNE can occur even for smaller grain size (0.76 mm) and fast flow velocities (>20 m d^{-1}). Shi et al. (2024) conducted numerical models and validated experimental data, suggesting the general LTNE criteria for a broader range of flow velocities. Their model showed that LTNE effects can occur in slow flow conditions for large grains. However, the

criteria are based on an empirical correlation for the heat transport coefficient, which is invalidated by experiments under groundwater conditions. Therefore, a better understanding of LTNE effects observed in two-phase heat transport experiments is required.

The aim of this work is to (a) analyze LTNE (i.e., the difference between fluid and solid temperature) observed in heat transport experiments by Lee et al. (2025) using two-phase numerical modeling in 2D, (b) investigate the influence of non-uniform flow in the porous media on LTNE effects through the model, (c) clarify the meaning of LTNE effects in porous media reflective of natural systems. We anticipate that our results can help to establish the conditions under which heat transport can be simplified to LTE in natural systems.

2. Material and Methods

2.1. Mathematical Description of Two-Phase Heat Transport in Porous Media

The present study combines LTE and LTNE models by coupling them with a heat transfer term. In the LTE model, water flow is described by *Darcy's law*, while heat transport is governed by the advection-diffusion equation in porous media. The equation is as follows (de Marsily, 1986):

$$\frac{\partial T}{\partial t} = D\nabla^2 T - v^t \cdot \nabla T, \tag{1}$$

where T is the temperature of the bulk porous medium (°C or K), t is the time (s), $D = \frac{\lambda}{\rho c}$ (m^2 $s{-}1$) is the bulk thermal dispersion coefficient, λ (W m^{-1} K^{-1}) is the thermal conductivity and ρc (J m^{-3} K^{-1}) is the volumetric heat capacity of the porous medium. v^t is the thermal front velocity (m s^{-1}) and is defined as:

$$v^t = q\frac{\rho_f c_f}{\rho c}, \tag{2}$$

where $q = -\frac{k}{\mu}\nabla p$ (m s^{-1}) is the *Darcy* velocity, with k (m^2) denoting the permeability, μ (Pa s) the dynamic viscosity, and p (Pa) the pore pressure. Permeability is defined as $k = K\frac{\mu}{\rho_f g}$, with K (m s^{-1}) denoting the hydraulic conductivity and g (m s^{-2}) the gravitational acceleration.

The thermal conductivity λ (W m^{-1} K^{-1}) and the volumetric heat capacity ρc (J m^{-3} K^{-1}) of the porous medium are (Bandai et al., 2023):

$$\lambda = n\lambda_f + (1-n)\lambda_s, \tag{3}$$

$$\rho c = n\rho_f c_f + (1-n)\rho_s c_s, \tag{4}$$

where n is porosity, λ_f and λ_s (W m^{-1} K^{-1}) are thermal conductivities and $\rho_f c_f$ and $\rho_s c_s$ are volumetric heat capacities (J m^{-3} K^{-1}) of fluid and solid phases, respectively.

A more precise description follows from separating the temperature in the fluid and solid phases and considering heat transfer between the phases (Amiri & Vafai, 1994). This approach is termed LTNE and is described by two energy equations coupled through a heat transfer coefficient h_{sf} (Kaviany, 1995; Levec & Carbonell, 1985b). In our study, we consider advective heat transport through a porous medium, for which the LTE assumption applies (Equation 1). This energy equation is coupled with the energy equation of the solid phase for heat conduction within a single grain. Unlike the common LTNE model of two energy equations for fluid and solid phases (Wakao & Kaguei, 1982), the porosity, n, is eliminated in both bulk and solid energy equations due to the spatial separation between two phases (Equations 5 and 6):

$$\rho c\frac{\partial T}{\partial t} + \rho c q\cdot\nabla T = \nabla\cdot(\lambda\nabla T) + h_{sf}a_{sf}(T_s - T), \tag{5}$$

$$\rho_s c_s\frac{\partial T_s}{\partial t} = \nabla\cdot(\lambda_s\nabla T_s) - h_{sf}a_{sf}(T_s - T), \tag{6}$$

where T and T_s (°C or K) are the temperatures of the fluid and solid phase, respectively. The heat transfer coefficient h_{sf} (W m^{-2}K^{-1}) is defined as the heat exchange across the specific surface area between the fluid and solid phase a_{sf} (m^{-1}):

$$h_{sf} = \frac{Nu\lambda_f}{d_p}, \tag{7}$$

where Nu is the dimensionless *Nusselt* number and d_p (m) is the grain diameter at the granular scale or the median of grain sizes at the larger scale. In our model, a_{sf} is defined as the interfacial area between the fluid and solid phases per unit bulk volume as follows:

$$a_{sf} = \frac{\pi d_p}{d_p^2} = \frac{\pi}{d_p}. \tag{8}$$

Here interfacial area is interfacial line defining the circular grain πd_p, while unit bulk volume is a square fitting exactly to the solid circle d_p^2. This allows upscaling of results from a single sphere to a porous medium with ideal packing.

2.2. Experimental Setup

This study employs experimental data from Lee et al. (2025), which we interpret using our advanced numerical model described in the following section. Lee et al. (2025) conducted specialized heat transport experiments to detect local thermal non-equilibrium (LTNE) effects in fully saturated porous media by independently measuring fluid and solid temperatures. Their experiments demonstrated a time-dependent temperature difference ($\Delta T(t)$) between phases that increases with both grain size and flow velocity. The temperature measurements were achieved by replicate LTNE probes. Each LTNE probe consists of a sphere with a temperature sensor at the center of the sphere for the solid phase and two temperature sensors on the right and left sides of the sphere, 2 mm away from the sphere for the fluid phase. Notably, the replicate LTNE probes under identical flow conditions produced $\Delta T(t)$ measurements with varying peak magnitudes.

To analyze these experimental results, we developed a numerical model matching Lee et al. (2025)'s experimental configuration. The laboratory flow-through heat transport experiments in a column are represented by thermal-hydraulic simulations in a square 2D domain with downward water and heat flow. The porous medium, consisting of 1 mm glass beads with embedded spheres for solid temperature measurement, is modeled as a homogenized porous medium under the local thermal equilibrium (LTE) assumption. The experimental temperature measurement spheres (with diameters of 5, 10, 15, 20, 25, and 30 mm) are represented by a central circular inclusion in our 2D model to capture solid-phase temperature behavior.

The simulations cover the experimental range of Darcy velocities (3–23 m d^{-1}). This 2D modeling approach successfully replicates the experimental measurement locations for both fluid and solid temperatures of LTNE probes while maintaining computational efficiency.

2.3. Numerical Modeling of Two-Phase Heat Transport Including Non-Uniform Flow

LTNE effects manifest as small temperature variations that are hidden in broader variations. In experimental settings, it is difficult to have good control over the boundary conditions, that is, inducing a perfect step change is impossible. Second, ambient temperature changes and water refill may affect the consistency of the input temperature signal. Third, the presence of non-uniform flow, as has been reported previously by Rau et al. (2012), can further confound the interpretation of temperature changes. These reasons render the use of analytical solutions to the two-phase heat transport problem impossible. Consequently, to allow quantitative analysis of the experimental temperature measurements, we deployed a numerical model. This permits inclusion of realistic boundaries and other artifacts. Additionally, a two-dimensional (2D) numerical model enables to define spatial position of temperature measurement for fluid and solid phases.

The thermal responses of the fluid and solid phases in the porous medium are obtained by solving the governing equations (Equations 5 and 6) using the open-source multiphysics simulation framework *Multiphysics Object-Oriented Simulation Environment* (MOOSE) (Harbour et al., 2025). This framework allows to numerically solve non-linear problems with multi-physics coupling using the finite element (FE) approach. We used the *Porous-Flow* module which is designed to enable coupled flow and heat transport through porous media with LTE assumption (Wilkins et al., 2021). Additionally, the *HeatConduction* module was used specifically for simulating the heat transfer within the solid phase. In the area of the background porous media, the LTE heat transport equations (Equation 5) are applied. The circular solid grain is spatially separated and only thermal diffusion (Equation 6) is resolved within the solid area (Figure 1). These two physics modules were coupled by a kernel *PorousFlowHeatMassTransfer*, which allowed heat transfer between fluid and solid phases through the inter-phase boundary. This kernel consists of two-phase temperature variables and a heat transfer term in the LTNE model including the local heat transfer coefficient h_{sf} and specific surface area a_{sf}. In our model, h_{sf} is locally defined only at the interface boundary, while the interface boundary is a line defining the solid circle, spatially separating it from the bulk volume of porous media. Increased thermal velocity by accelerated water flow next to a sphere was represented in the model.

The geometry of the domain was developed in 2D using *Gmsh* by reproducing the experiment column with a single sphere. In the numerical model, the bulk porous medium and the solid phase are defined separately by different mesh blocks. The spatial discretization was 0.001 m in the x and y directions. The mesh was refined at the boundary of the sphere and in the solid phase block with discretization of 0.0005 m. The number of elements consisting of the model domains was in the range between 343,816 and 373,728 depending on the grain size. The single sphere was defined as solid with only heat conduction, which is separated from the background porous medium, where the LTE-based advection-diffusion equation applies. To apply the LTNE model (Equations 5 and 6), heat conduction in the solid phase and heat flux within the porous medium were coupled using the heat transfer coefficient h_{sf} across the fluid-solid interface boundary (Equations 7 and 8). The model setting is illustrated in Figures 1a and 1b. The left and right boundaries were assigned to no-flow and no-heat-flux boundary conditions. Flow was modeled by applying a constant pore pressure difference between the top and bottom boundaries. The difference between top p_{top} and bottom pressure p_{bottom} per length of the model dx was computed for different *Darcy* velocities (q = 3, 8, 12, 17, 19, 23 m d^{-1}) as follows:

$$\frac{p_{\mathrm{top}} - p_{\mathrm{bottom}}}{dx} = q \cdot \frac{\mu}{k}. \tag{9}$$

The inlet temperature measurements ranging from initial temperature +5°C to +8°C (Table 1) were applied to the top boundary of the model to represent the heat input from the experiments. At the bottom of the model domain, constant initial temperature was applied. To predict LTNE effects based on experimental data, the LTNE probe, which consists of two temperature measurement points near the glass sphere located in the porous medium and one point at the center of the glass sphere (Lee et al., 2025), was replicated in the 2D numerical model. Parameter values and boundary conditions were assigned to the numerical model according to Table 1.

Previous experiments have illustrated that a non-uniform flow field occurring in homogeneous porous media can obscure small-scale heat transport processes (Lee et al., 2025; Rau et al., 2012). The phenomena are caused by locally created preferential flow pathways through the pore network within the porous media (Rau et al., 2012). This is an unavoidable side effect of experimentation and causes the thermal front to advance non-uniformly in the flow direction (Figure 2a). We embraced non-uniform flow in our model and developed a new but idealized approach to non-uniform flow simulation. Artificial non-uniform flow was simulated by varying the permeability of the porous medium along the x-direction, which leads to the horizontal variability in fluid flow around the central grain (Figure 2b). Permeability values ranging from 2×10^{-11} m^2 to 6×10^{-11} m^2 were applied to create different magnitudes of non-uniformity in the water flow. The slope of the thermal front induced by the permeability distribution created an unbalanced heat flow between the left and right sides of the 2D grain, as illustrated in Figures 2e–2g. This represents the horizontal temperature gradients in the surroundings of the grain, which is caused by non-uniform flow, while keeping the averaged Darcy flux unchanged for the non-uniform flow model scenarios with varied ω. In the porous media surrounding the circular solid phase, LTE model is applied. Thus, heat transfer coefficient is not defined in the domain where heterogeneous permeability is applied, but only at the interface between the solid sphere and the bulk porous medium.

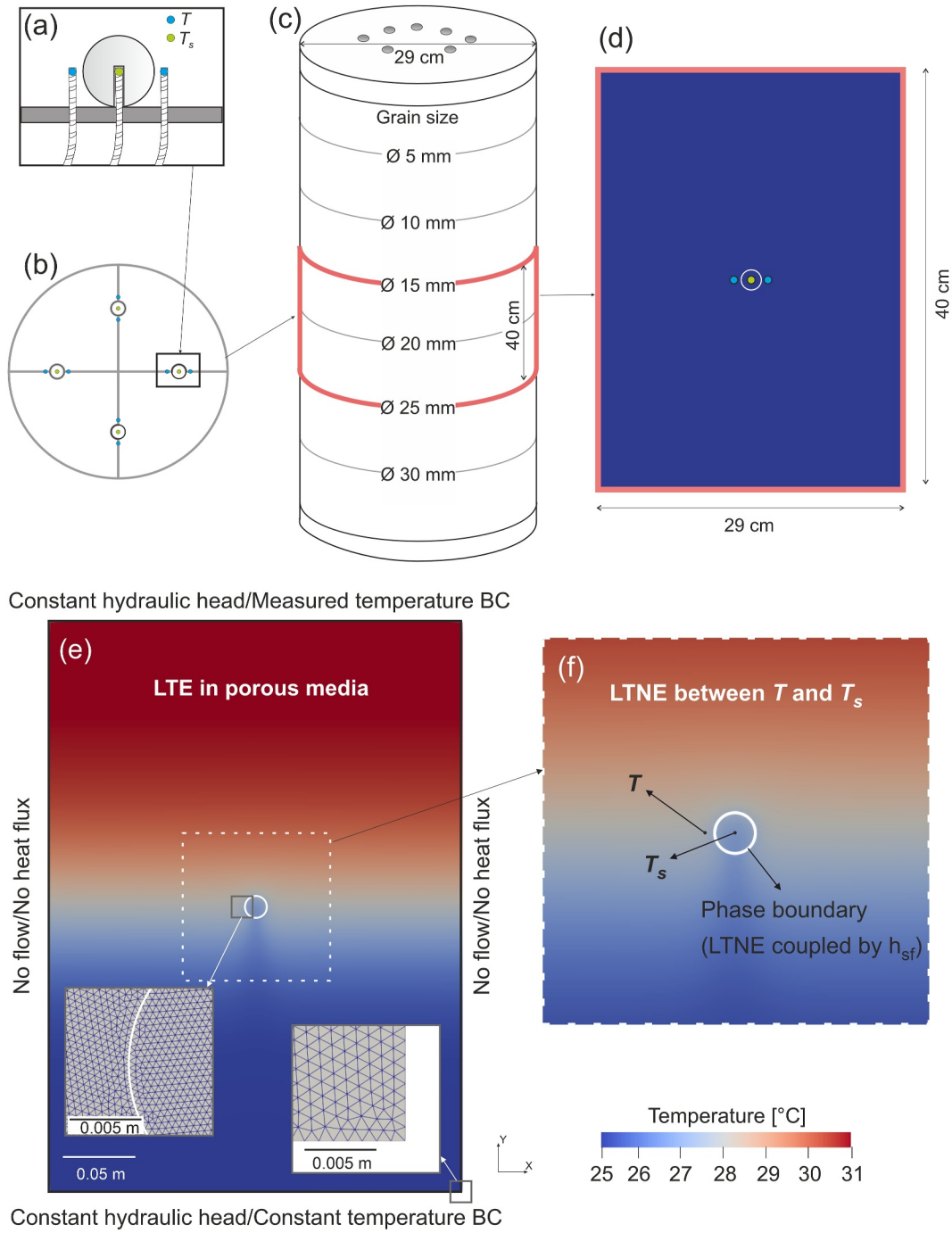

Figure 1. Experimental setup in Lee et al. (2025) and 2D numerical model. (a–c) Experimental setup, on which the conceptual model is based. (d) Conceptual model of one section of the experimental setup for one grain size. (e) Model domain defined with porous media for LTE heat transport and the separately defined solid phase at the center, with boundary conditions for the hydraulic and heat fluxes. (f) Zoomed-in model domain for LTNE heat transport indicating the coupled heat flux between fluid phase (T_f) and solid phase (T_s) at the phase boundary by heat transfer coefficient (h_{sf}).

2.4. Analysis of LTNE, Heat Transfer Coefficient, and Non-Uniform Flow

To validate our numerical LTNE model by reproducing the experimentally observed LTNE effects (Lee et al., 2025), the point value at 2 mm distance from the grain surface for the fluid phase and the point value at the center of the circular grain for the solid phase were used, corresponding to the measurement positions in

Table 1
Parameter Values and Boundary Conditions Assigned to the Numerical Model

Parameter	Value	Unit	Source
Initial temperature	24.18–33.56	°C	Lee et al. (2025)
Step heat input	+5–8	°C	Lee et al. (2025)
Porosity	0.37	-	Lee et al. (2025)
Thermal conductivity of fluid (20°C)	0.6	W m^{-1} K^{-1}	Wagner and Pruß (2002)
Thermal conductivity of solid	1.0	W m^{-1} K^{-1}	Lee et al. (2025)
Hydraulic conductivity	0.00323	m s^{-1}	Park and Lee (2021)
Permeability	2×10^{-11}–6×10^{-11}	m^2	Assumption
Darcy velocity	0.00004–0.000265	m s^{-1}	Lee et al. (2025)
Specific heat capacity of fluid	4,182	J kg^{-1} K^{-1}	Wagner and Pruß (2002)
Specific heat capacity of solid	759	J kg^{-1} K^{-1}	Lee et al. (2025)
Density of fluid	997	kg m^{-3}	Wagner and Pruß (2002)
Density of solid	2,585	kg m^{-3}	Lee et al. (2025)

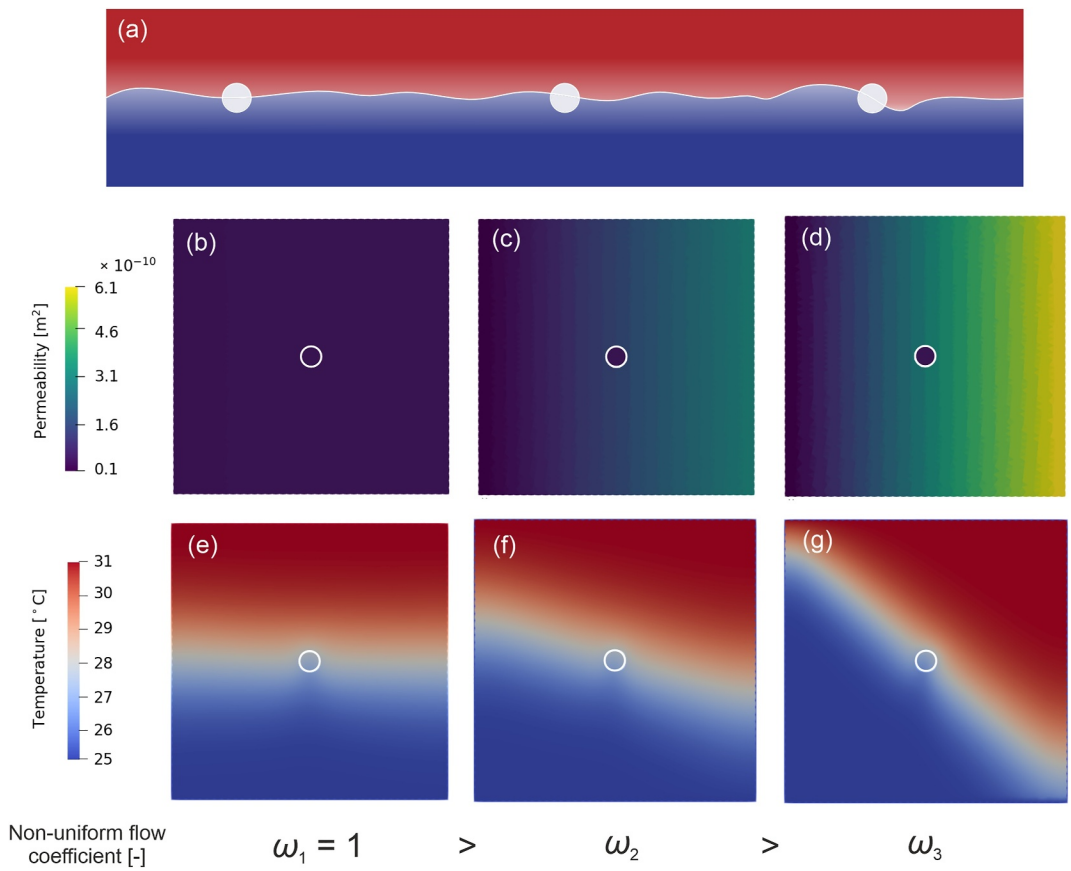

Figure 2. Non-uniform flow model integrated in the 2D numerical heat transport model. (a) Conceptual illustration of non-uniform flow in porous media. While each circle represents a grain embedded in homogeneous porous media, a curved horizontal line in the middle shows the thermal front influenced by non-uniform flow effects. (b–d) Three tested scenarios of permeability distribution applied in the non-uniform flow model to induce the change of thermal front slope along *x*-axis and manipulate the non-uniformity ω. (e–g) Visualized model results from heat transport simulation with the artificial non-uniform flow showing the tilted thermal front corresponding to the non-uniformity ω.

experiments by Lee et al. (2025). Temperature results are normalized by computing the difference between measured or modeled temperature and initial temperature and then dividing by final temperature in equilibrium. We adopt the LTNE definition from Levec and Carbonell (1985a, 1985b), where LTNE is expressed as the temperature difference between the fluid and solid phases:

$$\Delta T(t) = T(t) - T_s(t). \tag{10}$$

The resolution of normalized $\Delta T(t)$ is between 0.00125 and 0.002 as a result of the calculation by dividing the temperature sensor resolution of ±0.01 °C (Lee et al., 2025) by the temperature difference in the system (+5–8 K).

The value of the heat transfer coefficient h_{sf} in Equations 5 and 6 for the flow rates and textures under realistic hydrogeological conditions is unknown and untested. We therefore test the correlation of *Nusselt* number *Nu* by Gossler et al. (2020).

$$Nu = 1 + 3.1\mathrm{Re}^{0.57} \tag{11}$$

with experimental data. Here, Re is *Reynolds* number. In addition, h_{sf} is varied as a fitting parameter when fitting our model to the experimental results. This allows us to determine h_{sf} in the model to represent experimental LTNE effects. Although this correlation by Gossler et al. (2020) is based on experiments with extreme conditions in the field of engineering, it has been used to estimate h_{sf} for porous aquifers.

To quantify the magnitude of non-uniform flow at the grain scale, we develop a coefficient using the flow velocities as proxies for the arrival of the thermal front as follows:

$$\omega = \frac{v_{a,L}}{v_{a,R}}. \tag{12}$$

Here, $v_a = \frac{q}{n}$ is seepage velocities (m s^{-1}). The subscript L and R denote the left and right side of the sphere, respectively; $\omega = 1$ indicates uniform flow whereas $\omega < 1$ or $\omega > 1$ means non-uniform flow, with faster flow on one side compared to the other. We use this coefficient to attribute artifacts in the temperature breakthrough curves to non-uniform flow. Figure 2 shows how the arrival of the thermal front affects the value of ω.

3. Results

3.1. Match Between Experiments and Model and the Role of the Heat Transfer Coefficient

The results of 2D numerical simulations demonstrate that the model can accurately describe the local thermal non-equilibrium (LTNE) effects observed in laboratory heat transport experiments, as reported by Lee et al. (2025). The simulation results, using estimated heat transfer coefficient by the empirical correlation (Equation 11) or fitting by increasing heat transfer coefficient, show the temperature rise due to a step-like heat input for both phases over time. These results align well with experimental data for spheres ranging from 5 to 20 mm in diameter.

For instance, Figures 3a and 3b illustrates that the thermal breakthrough curves (BTCs) generated by the model with empirical h_{sf} closely match the experimental BTCs for a grain size of 20 mm. However, for larger grain sizes of 25 and 30 mm, the modeled BTCs of the solid phase rise later than the experimental BTCs when simulations are performed with the correlation-based estimate of heat transfer coefficient (Equations 7 and 11) (Figure 3).

To fit the model closer to the experimental data, the maximum possible heat transfer coefficient of 10^8 W m^{-2} K^{-1} was applied. The maximum possible heat transfer coefficient is the largest value that enables the convergence of the numerical solution. The model results using the maximum h_{sf} show only a slight improvement in fitting compared to the model results using the empirical h_{sf}, reducing the RMSE by less than 0.0002. This is demonstrated in Figures 3a–3d, by BTCs with maximum h_{sf} in dark red, aligned with BTCs with empirical h_{sf} in light pink. With the maximum value of h_{sf}, the unlimited heat transfer between the fluid and solid phases with maximum h_{sf} allowed immediate heat flux through the phase boundary between two phases (Figures 3e and 3f).

10.1029/2025WR041260

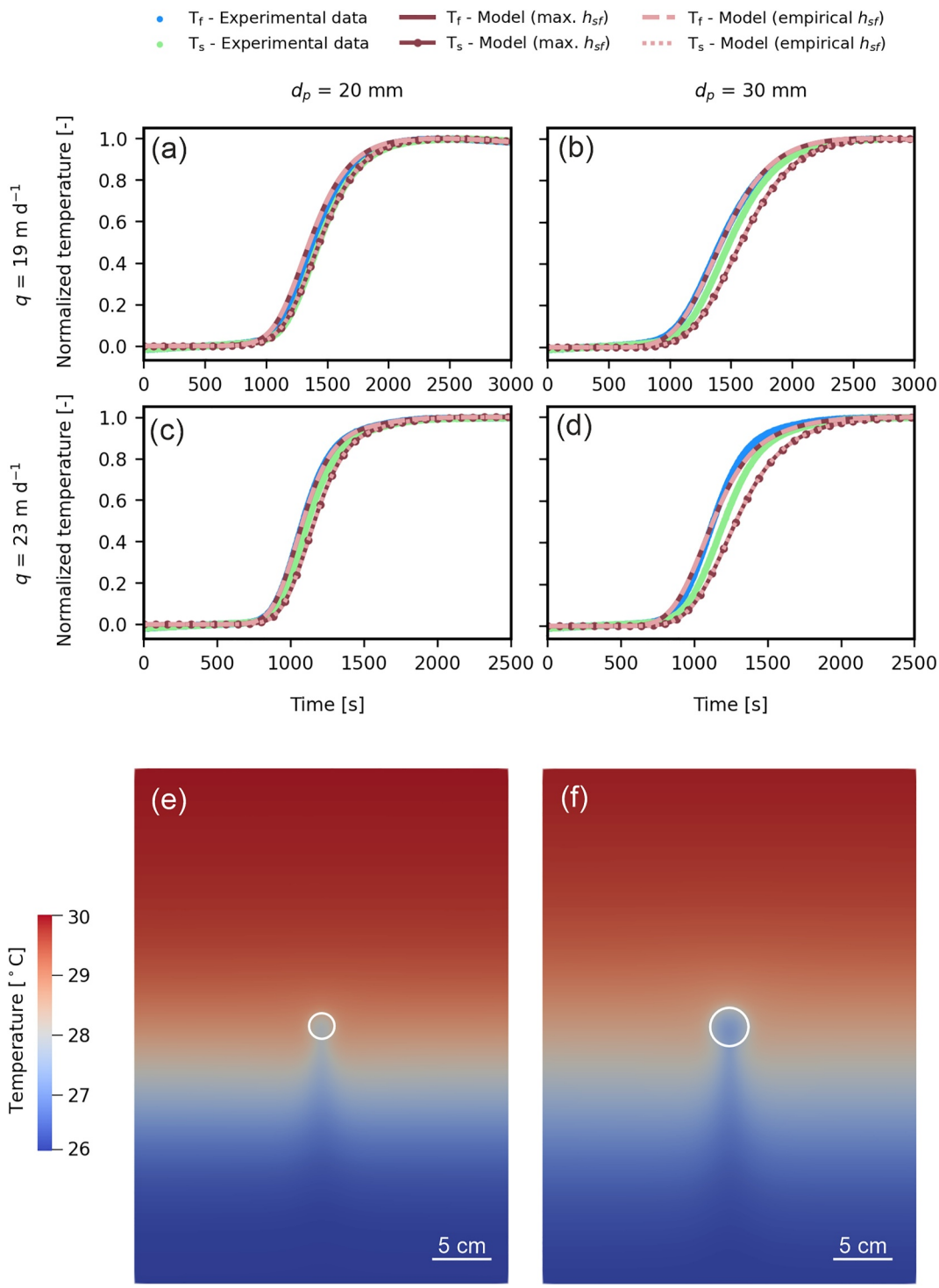

Figure 3. Comparison between experimental data and model results with the estimated heat transfer rate by a correlation and unlimited heat transfer. Blue and green dots represent temperature measurement of fluid (T_f) and solid phases (T_s), respectively. Dark red solid and dashed lines show model results with empirical h_{sf}), while pink solid and dashed lines present model results with maximum h_{sf}. (a, b) Thermal breakthrough curves (BTCs) for fluid and solid phases from experimental data and model results with Darcy flux of 19 m d^{-1} for two different grain sizes. (c, d) BTCs for each phase from experimental data and model results with Darcy flux of 23 m d^{-1} for two different grain sizes. (e, f) Model output with Darcy flux of 23 m d^{-1} and the maximum heat transfer coefficient, max. h_{sf}, showing temperature profile in the domain for grain size of 20 and 30 mm.

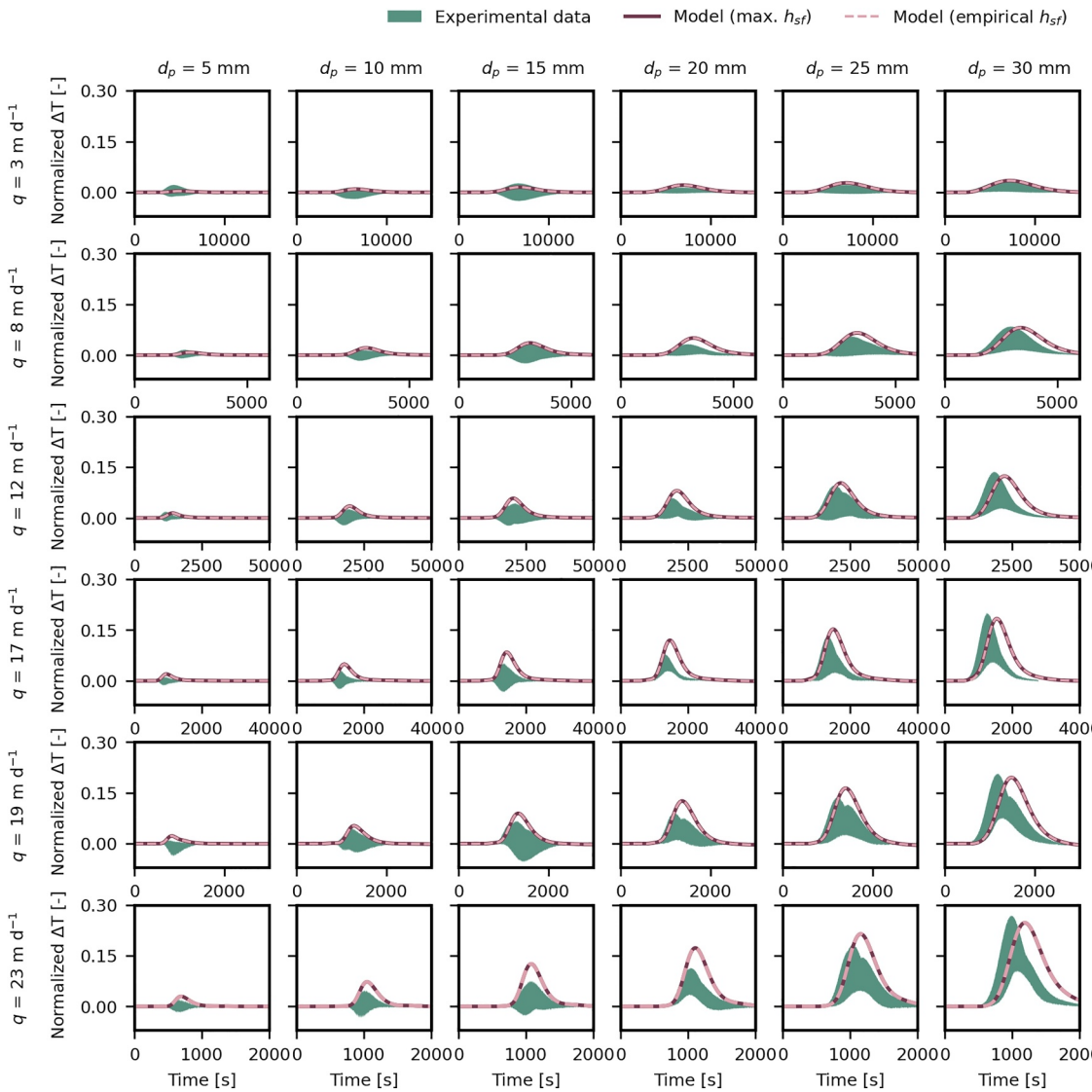

Figure 4. Summary of experimental data and model results with estimated heat transfer coefficient, empirical h_{sf}, and the possible maximum heat transfer coefficient, max. h_{sf}, for six different grain sizes and six different flow velocities. The green shaded area demonstrates the range between minimal and maximal ΔT(t) measured for a specific grain size and a specific flow velocity from the laboratory experiments by Lee et al. (2025). The pink dashed line indicates the ΔT(t) range from the model results with the estimated empirical h_{sf} by the correlation of Gossler et al. (2020). The dark red solid line presents the modeled ΔT(t) with max. h_{sf}.

3.2. Local Thermal Non-Equilibrium Effects

Our LTNE model captures the largest magnitude of LTNE observed in experiments by Lee et al. (2025). In Figure 4, the modeled $\Delta T(t)$ curves with empirical h_{sf} and max. h_{sf}, shown in light pink and dark red, respectively, align well with the experimental $\Delta T(t)$ curves, particularly matching the highest peak within the green shaded area of the experimental $\Delta T(t)$ range. As flow velocity increases, the modeled $\Delta T(t)$ curves tend to exhibit higher or shifted peaks compared to the experimental data range. This trend is also observed with increasing grain sizes, where the modeled $\Delta T(t)$ curves show larger discrepancies from the experimental range for larger grain sizes. The shifted $\Delta T(t)$ curves for larger grain sizes are resulted from the delayed rise of BTCs of the solid phase, as shown in Figures 3b and 3d. Notably, for a grain size of 30 mm, the modeled $\Delta T(t)$ reaches the maximum experimental $\Delta T(t)$ by reducing the heat transfer coefficient h_{sf} to a value smaller than the empirical h_{sf}. However, the lowest boundary of experimental $\Delta T(t)$ could not be achieved by adjusting h_{sf}. Increasing h_{sf} to its maximum possible value did not affect the $\Delta T(t)$ curves significantly, as shown by overlapping $\Delta T(t)$ with empirical $\Delta T(t)$ and max.

h_{sf} in Figure 4. Consequently, varying h_{sf} does not produce the inverse pulse of $\Delta T(t)$ (i.e., negative ΔT) that are observed in the experiments.

3.3. Non-Uniform Flow and Reduced Dimensionality of Modeling

As described earlier, the model results could not capture the experimental $\Delta T(t)$ with smaller peaks from other replica measurements under the same conditions. Furthermore, the LTNE model with an ideally uniform flow condition failed to reproduce the inverse pulses from negative $\Delta T(t)$ values, indicating delayed thermal arrival in the fluid phase. As hypothesized in Lee et al. (2025), the inverse pulse can be attributed to non-uniform flow effects. Therefore, without incorporating non-uniform flow effects, the model consistently shows positive $\Delta T(t)$ (Figure 4). This limitation in describing the observed LTNE effects from experiments led to the development of non-uniform flow modeling. This approach allows the heat transport model to account for unexpected $\Delta T(t)$ values that arise under non-uniform flow conditions.

This new non-uniform flow simulation approach, performed using a 2D model in MOOSE, produced an inclined thermal front along the x-direction that increased thermal velocities along the axis in the model domain. Consequently, the model resulted in a lower fluid temperature on the left side of a grain compared to the solid temperature at the grain's center (Figure 2). This led to a preceding BTC of the solid phase compared to the fluid phase, thereby demonstrating a reduced peak in the $\Delta T(t)$ curves by solid red lines in Figures 5c and 5d and Figures g–h. On the other hand, dashed red lines in the figures present enhanced peaks of $\Delta T(t)$ curves resulted from comparison between the fluid temperature on the right side of a grain and the solid temperature.

The 2D numerical model, incorporating the simplified artificial non-uniform flow, influenced the $\Delta T(t)$ curves by either faster or slower advective heat transport. The effects demonstrate intensified or hindered LTNE effects by non-uniform flow. The model results show that the modeled $\Delta T(t)$ curves can lie within the range of experimental $\Delta T(t)$. These results are presented in Figure 5, which shows that decreasing ω either reduces or increases the peak of the modeled $\Delta T(t)$ curves, depending on whether the left or right side adjacent to the solid grain is considered. Especially, integrating the non-uniform flow model into the LTNE model enabled the simulation of inverse peaks in $\Delta T(t)$. These inverse peaks align with the experimental $\Delta T(t)$ observed for grain sizes between 5 and 15 mm, as shown in Figures 5c and 5g. However, for the larger grain size of 15 mm, the non-uniform flow model with the same permeability distribution did not always produce $\Delta T(t)$ within the experimental range, as shown in Figures 5d and 5h.

4. Discussion

4.1. Numerical LTNE Model Including Non-Uniform Flow Reveals Exacerbated Thermal Non-Equilibrium

Compared to the state-of-the-art analytical models used by Lee et al. (2025), our new model results demonstrate an improved match of the temperature breakthrough curves (BTCs) observed in laboratory experiments. This is evident in the steeper rise and the spread-out tail of the BTCs, which better align with the experimental BTCs compared to the 1D LTNE model of Lee et al. (2025), which fails to describe experimental BTCs for grain sizes between 20 and 30 mm. While the BTCs of the fluid phase are well described by the model with maximum h_{sf} or empirical h_{sf} ($RMSE < 0.02$), the modeled BTCs of the solid phase show a larger discrepancy (e.g., by $RMSE < 0.06$) compared to the model with the same h_{sf} for the fluid phases (Figure 3). This discrepancy could be attributed to the measurement uncertainty of the thermal conductivity and the volumetric heat capacity of the solid phase.

Our new model includes boundary conditions from inlet temperature measurements, allowing it to represent the non-ideal heat input from the experiments. This improves the description of experimental LTNE effects. Additionally, the two-dimensional nature of the model enables accurate spatial separation of fluid and solid phases within the modeling domain. Consequently, detailed and fully coupled physics are applied to each phase via the heat transfer coefficient at the phase boundary. While the LTNE magnitude is well predicted by our model, the modeled solid phase temperature for larger grain sizes shows a delayed rise compared to the measured solid temperature in experiments (Figure 3). This can be attributed to the stronger influence of solid phase thermal properties and their measurement uncertainties for the larger grains. The thermal conductivity of the solid phase could enforce LTNE effects. This aligns with the parametric study of the LTNE model including λ_s and $\rho_s c_s$ by

10.1029/2025WR041260

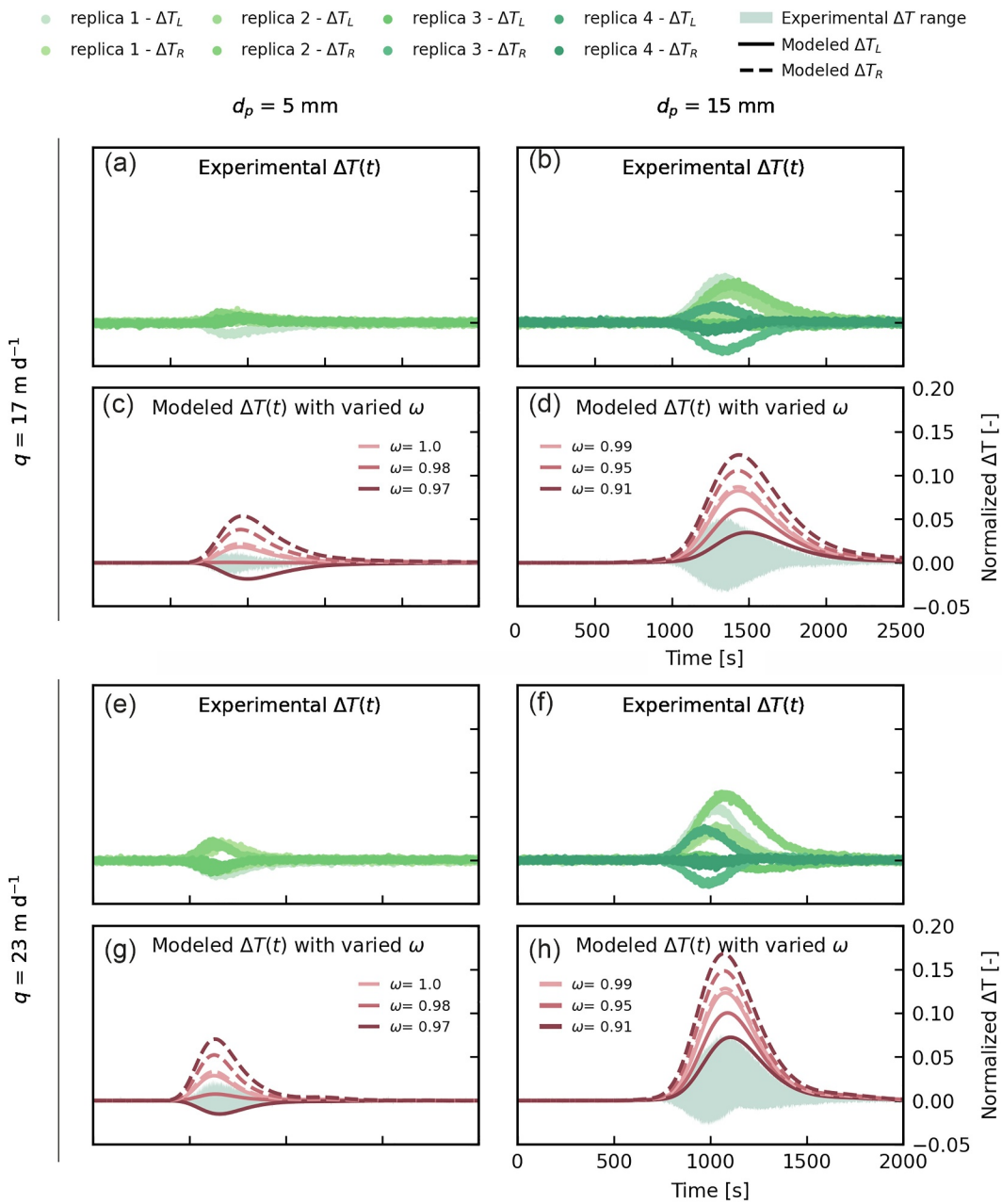

Figure 5. Comparison between experimental data and non-uniform flow model results for two different grain sizes (5 and 15 mm diameter) and two different flow velocities. The subscript L and R indicate if the fluid temperature is measured or modeled on the left (L) or right side (R) of a grain to compute ΔT(t). The maximum heat transfer coefficient is applied in the model. (a, b) Experimental ΔT(t) for Darcy flux of 17 m d^{-1} and two grain sizes (green dots). (c, d) Modeled ΔT(t) with varied non-uniform flow coefficient ω on the left side (solid red lines) and on the right side of the grain (dashed red lines) with a Darcy flux of 17 m d^{-1} for two different grain sizes comparing to the experimental data (green shaded area). (e, f) Experimental ΔT(t) for a Darcy flux of 23 m d^{-1} and two grain sizes shown by green dots. (g, h) Modeled ΔT(t) with varied ω with a Darcy flux of 23 m d^{-1} for two grain sizes comparing to the experimental data.

Bandai et al. (2023). Their work shows that decreasing $\rho_s c_s$ and increasing λ_s reduces the peak of ΔT between the fluid and solid phases, implying a smaller discrepancy between the BTCs of the two phases. In our model results, a colder temperature tail appears beneath the defined solid phase, particularly in Figures 3e and 3f. This feature arises from fluid flow around the circular grain, where a stagnation point forms below the solid phase.

Non-uniform flow effects have previously been reported during heat transport experiments in a homogeneous system (Rau et al., 2012) and as a factor obscuring LTNE effects (Bandai et al., 2017; Gossler et al., 2019; Lee et al., 2025). For example, Lee et al. (2025) observed inverse pulses in $\Delta T(t)$ that were hypothesized to be caused by a non-uniform flow field. Our model results consider such non-uniform flow and show that the inverse pulse of $\Delta T(t)$ are indeed created by a small flow non-uniformity ($\omega = 0.97$) for a grain size of 5 mm. Additionally, a greater increase or reduction of the $\Delta T(t)$ peak for the small grain ($d_p = 5$ mm) is demonstrated in comparison to the one for a larger grain ($d_p = 15$ mm) with the same change of non-uniformity (ω). This explains why experimental $\Delta T(t)$ only for small grain sizes from 5 to 15 mm shows inverse pulses, as this phenomenon may have a stronger effect in a smaller *Representative Elementary Volume* (*REV*) at the small scale in homogeneous porous media.

While modeled non-uniform flow can reduce the magnitude of the LTNE effect or reverse the thermal arrival time between fluid and solid phases, it can also intensify LTNE effects by increasing the peak of $\Delta T(t)$. This implies that the observed LTNE effects can result from thermal disequilibrium due to limited heat transfer between the two phases and from a transverse thermal gradient introducing lateral spreading of heat within the porous media (Rau et al., 2012). Such effects are not accounted for in analytical models and clearly necessitate more advanced modeling approaches such as ours.

Overall, our numerical model successfully explains experimental observations and confirms existing hypotheses of the presence of a non-uniform flow field during flow through homogeneous porous media. We further note that our 2D LTNE numerical model successfully represents the observed LTNE effects in laboratory experiments under typical conditions found in hydrogeology. However, we anticipate that flow non-uniformity will be exacerbated in groundwater systems that are naturally heterogeneous.

While heat transfer between fluid and solid phases is a key driver of LTNE in groundwater flow problems, our 2D numerical model provides two-phase heat transport capabilities, enabling investigation of detailed fluid-solid interactions at the granular scale. The model, validated against experiments, can predict heat transport within the smallest representative elementary volume by isolating a single grain from the surrounding fluid. This framework allows systematic testing of granular-scale heat transport under varying grain sizes and hydraulic and thermal properties. In addition, the model reveals the mechanisms behind LTNE effects, highlighting how different treatments of two-phase porous media influence heat transfer.

4.2. Heat Transfer Coefficient for Two-Phase Transient Heat Transport

Previous studies in mechanical and chemical engineering have explored various two-phase transient heat transport models (Kaviany, 1995; Wakao & Kaguei, 1982). Especially, the simplified models were addressed by Wakao et al. (1979), such as the Schumann model, the continuous solid phase (C-S) model, and the dispersion concentric (D-S) model. These models use a heat transfer coefficient to describe heat transfer between phases and predict heat transport in porous media under specific conditions (Wakao et al., 1979). The C-S model is commonly used in the literature to account for axial heat conduction in the solid phase along the flow direction. While Lee et al. (2025) utilized the C-S model for 1D numerical solution, their numerical model failed to represent the LTNE effects observed in their laboratory experiments. Although they applied the empirical correlation of h_{sf} by Gossler et al. (2020), it could not be tested by their model. Our results demonstrate that $\Delta T(t)$ is not affected by varying heat transfer coefficient from an estimated empirical value to the possible maximum value (Figure 4). It indicates that a sufficiently large h_{sf} ensures unobstructed heat transfer between the fluid and solid phases, accurately representing the experimental LTNE effects. $\Delta T(t)$ is clearly insensitive to values of h_{sf} that exceed previous estimates under conditions typical for groundwater systems.

According to the model results from Lee et al. (2025) and the present study, the estimated heat transfer coefficient obtained through fitting procedures can vary depending on the model dimension. The larger specific surface area in the 3D model, which is defined as the ratio of surface area to volume of a sphere, $a_{sf} = \frac{6}{d_p}$ (m^{-1}), compared to the one of 2D model could influence a heat transfer rate between the fluid and solid phases in an elementary volume. However, the difference between values of a_{sf} in 2D and 3D is relatively small compared to the potential value range of heat transfer coefficients that illustrate negligible change in $\Delta T(t)$. For example, while a_{sf} in 3D is 1.5 times larger than a_{sf} in 2D, the heat transfer coefficient variation range comprises a factor of 10^7. Due to the

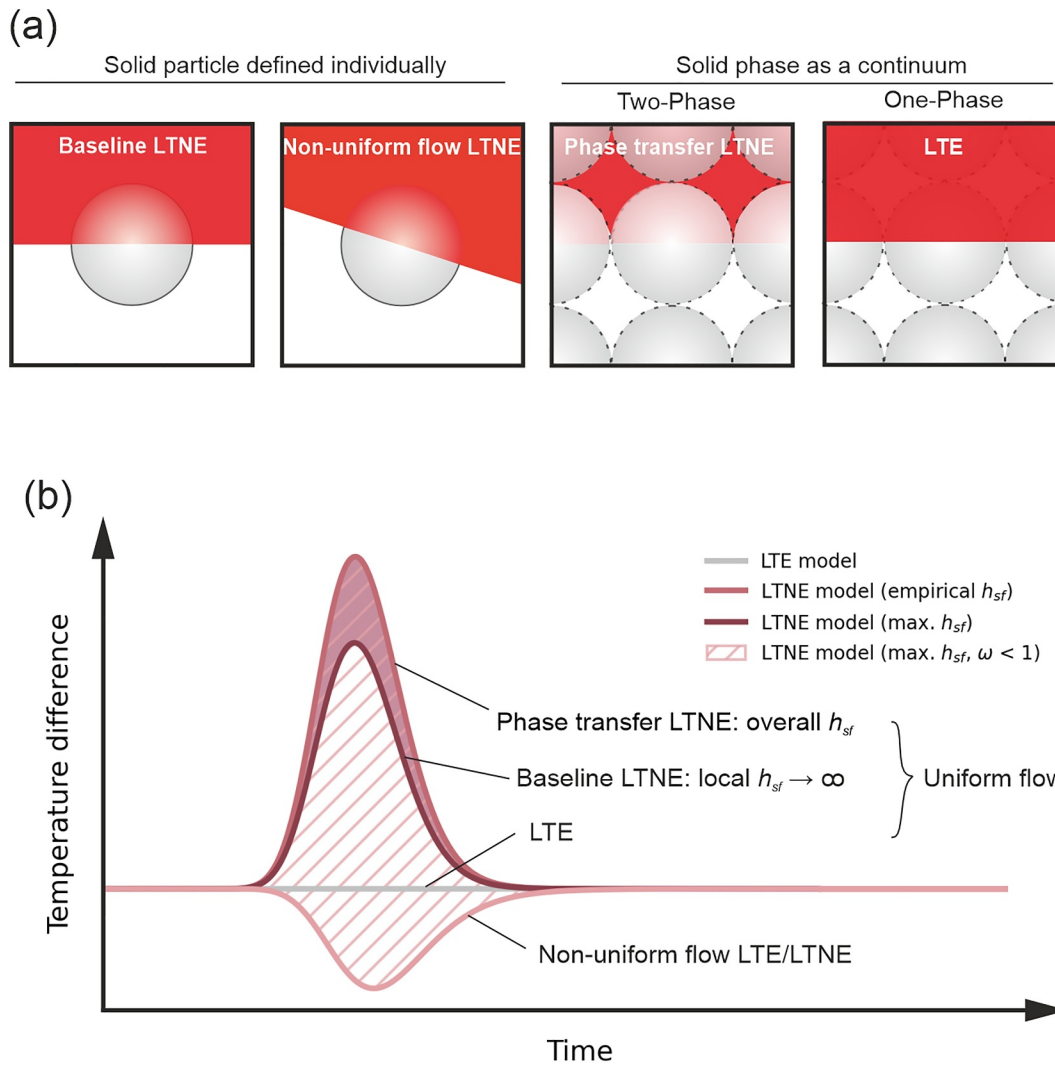

Figure 6. (a) Illustration of four concepts of heat transport in porous media, which can be distinguished by different $\Delta T(t)$ patterns derived from temperature difference between fluid (T_f) and solid phase (T_s) induced by heat input from the top (red shaded area). (b) Conceptual demonstration of $\Delta T(t)$ patterns for each concept of heat transport in porous media. Under uniform flow conditions, either LTE (gray line) or LTNE with a positive $\Delta T(t)$(t) can occur. $\Delta T(t)$ may lie between baseline LTNE (dark red line) and phase transfer LTNE (pink line), as illustrated by the teal shaded area. A temperature difference between T_f and T_s can also arise from non-uniform flow (light pink line), which may present as an inverse pulse of $\Delta T(t)$ or a positive $\Delta T(t)$ across the hatched area by non-uniform flow LTNE model with varied non-uniformity.

parameter scale, it is clear that the possible change of a_{sf} for 3D conditions would not affect the interface heat transfer significantly. This leads us to conclude that our 2D model is sufficient to predict LTNE effects.

4.3. Heat Transport in Porous Media at the Granular Scale Can Be Attributed to Different Concepts

The temperature difference between fluid and solid phases indicates the intensity of local thermal non-equilibrium (LTNE) within porous media. Our advanced model, which incorporates mixed thermal processes through heat flux in both phases, provides detailed insights into LTNE effects. We propose that four key concepts should be considered to understand heat transport in porous media: (a) thermal disequilibrium due to different thermal properties between fluid and solid phases (max. h_{sf}), (b) non-uniform flow, (c) interphase heat transfer when h_{sf} has small values (h_{sf} < empirical h_{sf}) that limit heat transfer between phases, and (d) local thermal equilibrium (LTE) which unifies both phases and is generally used. Figure 6 summarizes these concepts using $\Delta T(t)$ as a

measure. Baseline LTNE is the case when the solid is defined individually, considering $T_f = T_s$ at the interface boundary, as shown by model results in the present study. Phase transfer LTNE occurs when the solid phase is treated as a continuum, considering the fact that volume-averaged temperatures of the fluid and solid phases are not equal within the representative elementary volume of the porous media.

Due to the differences in thermal properties between fluid and solid phases, thermal arrival mismatch between phases can occur, demonstrating the baseline $\Delta T(t)$ with maximum heat transfer between phases in the model. As heat transfer is maximized at the boundary of the two phases, the delayed heat flux of the solid phase can be attributed solely to the thermal properties of the solid phase in the model.

When limited heat transfer between fluid and solid phases at the phase boundary is hypothesized, LTNE effects can be intensified by a reduced heat transfer coefficient. This can create a $\Delta T(t)$ with a higher peak than the baseline LTNE, a phenomenon we refer to as *phase transfer LTNE*. However, the aforementioned LTNE can occur even with the assumption of uniform flow in the porous media.

When non-uniform flow is considered, LTNE effects can be either intensified or suppressed by the transversely non-uniform thermal front. This can mask the thermal disequilibrium caused by interphase heat transfer. Based on this, we can assume that experimental LTNE with a peak $\Delta T(t)$ as large as or similar to the baseline LTNE peak could be a consequence of LTNE due to non-uniform flow effects or LTE influenced by non-uniform flow field.

4.4. Implications for Heat Transport Modeling From Granular to Field Scales

Understanding LTNE effects at the granular scale is crucial for characterizing thermal processes that can be upscaled through effective thermal parameters. While previous studies have simulated LTNE effects using homogenized porous media models based on granular-scale experiments (Bandai et al., 2023; Lee et al., 2025), their 1D LTNE models failed to accurately capture experimental observations, likely due to unaccounted non-uniform flow effects.

Our 2D two-phase LTNE model successfully reproduces experimental LTNE effects when incorporating unlimited interface heat transfer (baseline LTNE). As demonstrated by the comparable modeled LTNE with empirical h_{sf} and the modeled LTNE with unlimited heat transfer, LTNE induced by obstructed heat transfer may not be significant at the granular scale. Therefore, phase transfer LTNE should be considered for the larger scales. Although our study focuses on heat transfer at the granular scale, the conceptual regimes we identify highlight the main drivers for LTNE depending on how the two-phase porous media is represented. When the solid phase is modeled as a single grain separated from the fluid, LTNE is mainly limited by the strong thermal gradient within the grain itself (Baseline LTNE). In contrast, for a realistic porous medium with many grains, the system can be treated as a continuum, where LTNE is limited by the overall convection heat transfer coefficient within the representative volume (Phase transfer LTNE). More importantly, we demonstrate that flow field heterogeneity can obscure intrinsic LTNE effects arising from the two-phase nature of porous media. This explains why models assuming ideal uniform flow perform poorly in predicting LTNE (Bandai et al., 2023; Lee et al., 2025), particularly given the inevitable flow non-uniformity in homogeneous porous media (Rau et al., 2012). These findings suggest that LTNE observed in natural systems may be based on baseline LTNE modified by flow heterogeneity effects at the granular scale. Such effects will be stronger in natural environments where heterogeneity of grain sizes increases flow non-uniformity and variability of thermal gradient within the solid phase.

LTNE can be understood at different scales. The Figure 6 shows that at the granular scale, LTNE arises either from heat conduction within the solid phase or from non-uniform flow patterns. This aligns with the quantitative evaluation of LTNE by Lee et al. (2025). At the continuum scale, however, LTNE should be considered as the temperature difference between volume-averaged fluid and solid phases within the representative elementary volume. Future studies will be needed to quantify LTNE at this scale using volumetric temperatures of both phases.

At the granular scale, LTNE manifests as fluid-solid temperature differences ($\Delta T(t)$). Our results reveal that flow non-uniformity can amplify $\Delta T(t)$ or even generate inverse thermal pulses (negative $\Delta T(t)$). Previous laboratory studies testing LTE assumptions treated homogeneous media as single continua with averaged thermal properties (Baek et al., 2022; Gossler et al., 2019). These studies compared apparent versus effective thermal retardation

factors, finding general agreement at moderate velocities but increasing deviations at higher flows - a phenomenon attributed to non-uniform flow effects (Baek et al., 2022).

Field-scale heat transport models typically employ single-phase formulations assuming LTE, where non-uniform heat transport emerges from hydraulic conductivity heterogeneity (Hoffmann et al., 2019; Irvine et al., 2015; Schornberg et al., 2010). Our findings suggest that field-scale LTNE-like effects may similarly originate from flow heterogeneity. As shown by Gebhardt et al. (2025), such effects due to large-scale variations in hydraulic conductivity are quantifiable through differences between effective and apparent thermal retardation factors. This connection bridges granular-scale LTNE mechanisms with field-scale thermal transport phenomena. Although in the natural systems at the field scale, many additional factors, such as multi-phase transport, biochemical reaction, and micro-scale variation in flow characteristics, are involved in heat transport, the present study focuses on the detailed heat transfer mechanisms of LTNE effects by simplifying the processes in our advanced model for practical use.

In the natural systems, porous media are treated as a continuum using a volume-averaged approach within the representative elementary volume. This averaging smooths out thermal gradients within individual grains, thereby neglecting baseline LTNE. We therefore interpret continuum scale LTNE effects as the combined result of three mechanisms: (a) grain-scale heat conduction within solid particles (baseline LTNE), (b) convective heat transfer between fluid and solid driven by advective flow, and (c) non-uniform flow along preferential pathways. In the volume-averaged framework, granular-scale LTNE effects are embedded in lumped parameters: non-uniform flow is represented through hydrodynamic dispersion, while convective transfer (Nusselt number) and grain-size-dependent baseline LTNE are captured by the overall heat transfer coefficient.

5. Conclusions

We developed and validated a novel numerical model for two-phase heat transport that incorporates heat transfer between phases and non-uniform flow effects. The model was applied to analyze previously published experimental data on local thermal non-equilibrium (LTNE), revealing that experimentally observed LTNE effects - quantified by the transient solid-fluid temperature difference $\Delta T(t)$ - are predominantly dominated by flow non-uniformity. This phenomenon obscures other contributing factors to LTNE, such as contrasts in thermal properties and interfacial heat transfer rates between phases.

Our findings provide granular-scale insights into LTNE mechanisms in porous media, demonstrating that LTNE can arise from either dissimilar thermal properties between phases or non-uniform flow. From this analysis, we define four conceptual regimes that govern heat transport at the granular scale: (a) baseline LTNE under uniform flow, (b) LTE/LTNE under non-uniform flow, (c) phase-transfer-driven LTNE under uniform flow, and (d) local thermal equilibrium (LTE) under uniform flow.

These four regimes describe heat transport in porous media while considering heat transfer processes and granular-scale flow conditions. LTE with idealized uniform flow yields zero interphase temperature difference. Baseline LTNE is captured when applying an infinite heat transfer coefficient ($h_{sf} = 10^8$ W m^{-2} K^{-1}), matching experimental data. The model using the empirical coefficient from Gossler et al. (2020) also predicts the experimental LTNE effects closely, demonstrating a negligible phase-transfer-driven LTNE. Most notably, incorporating flow non-uniformity explains why experiments often measure attenuated LTNE effects: flow variations either amplify or counteract inherent LTNE, complicating the identification of underlying mechanisms.

Future studies should prioritize two advancements: (a) Engineered porous media with perfectly ordered packing to suppress flow non-uniformity, enabling precise heat transfer coefficient determination, and (b) high-resolution 3D heat transport models that explicitly resolve granular geometry and pore-scale flow paths including non-uniform flow. Such approaches will further elucidate the coupled roles of microstructure and transport physics in two-phase thermal systems.

Conflict of Interest

The authors declare no conflicts of interest relevant to this study.

Data Availability Statement

The scripts and code used for the model and the analysis are available at Zenodo (https://doi.org/10.5281/zenodo.17330106) (Lee, 2025).

Acknowledgments
This project has received funding from the German Research Foundation (DFG) grant agreement number 468464290. We would like to thank Andy Wilkins for the support with the numerical model software. We would like to thank the helpful comments of the editors, Wenguang Shi, and the anonymous reviewers. Open Access funding enabled and organized by Projekt DEAL.

References

Amiri, A., & Vafai, K. (1994). Analysis of dispersion effects and non-thermal equilibrium, non-Darcian, variable porosity incompressible flow through porous media. *International Journal of Heat and Mass Transfer*, *37*(6), 939–954. https://doi.org/10.1016/0017-9310(94)90219-4

Anibas, C., Tolche, A. D., Ghysels, G., Nossent, J., Schneidewind, U., Huysmans, M., & Batelaan, O. (2018). Delineation of spatial-temporal patterns of groundwater/surface-water interaction along a river reach (Aa River, Belgium) with transient thermal modeling. *Hydrogeology Journal*, *26*(3), 819–835. https://doi.org/10.1007/s10040-017-1695-9

Baek, J.-Y., Park, B.-H., Rau, G. C., & Lee, K.-K. (2022). Experimental evidence for local thermal non-equilibrium during heat transport in sand representative of natural conditions. *Journal of Hydrology*, *608*, 127589. https://doi.org/10.1016/j.jhydrol.2022.127589

Bandai, T., Hamamoto, S., Rau, G. C., Komatsu, T., & Nishimura, T. (2017). The effect of particle size on thermal and solute dispersion in saturated porous media. *International Journal of Thermal Sciences*, *122*, 74–84. https://doi.org/10.1016/j.ijthermalsci.2017.08.003

Bandai, T., Hamamoto, S., Rau, G. C., Komatsu, T., & Nishimura, T. (2023). Effects of thermal properties of porous media on local thermal (non-) equilibrium heat transport. *Journal of Groundwater Hydrology*, *65*(2), 125–139. https://doi.org/10.5917/jagh.65.125

de Marsily, G. (1986). *Quantitative hydrogeology: Groundwater hydrology for engineers*. Academic.

Di Dato, M., D'Angelo, C., Casasso, A., & Zarlenga, A. (2022). The impact of porous medium heterogeneity on the thermal feedback of open-loop shallow geothermal systems. *Journal of Hydrology*, *604*, 127205. https://doi.org/10.1016/j.jhydrol.2021.127205

Gebhardt, H., Zech, A., Rau, G. C., & Bayer, P. (2025). Effective thermal retardation in aquifers of heterogeneous hydraulic conductivity. *Water Resources Research*, *61*(10), e2025WR040153. https://doi.org/10.1029/2025WR040153

Gossler, M. A., Bayer, P., Rau, G. C., Einsiedl, F., & Zosseder, K. (2020). On the limitations and implications of modeling heat transport in porous aquifers by assuming local thermal equilibrium. *Water Resources Research*, *56*(10), e2020WR027772. https://doi.org/10.1029/2020WR027772

Gossler, M. A., Bayer, P., & Zosseder, K. (2019). Experimental investigation of thermal retardation and local thermal non-equilibrium effects on heat transport in highly permeable, porous aquifers. *Journal of Hydrology*, *578*, 124097. https://doi.org/10.1016/j.jhydrol.2019.124097

Hamidi, S., Heinze, T., Galvan, B., & Miller, S. (2019). Critical review of the local thermal equilibrium assumption in heterogeneous porous media: Dependence on permeability and porosity contrasts. *Applied Thermal Engineering*, *147*, 962–971. https://doi.org/10.1016/j.applthermaleng.2018.10.130

Harbour, L., Giudicelli, G., Lindsay, A. D., German, P., Hansel, J., Icenhour, C., et al. (2025). 4.0 MOOSE: Enabling massively parallel multiphysics simulation. *SoftwareX*, *31*, 102264. https://doi.org/10.1016/j.softx.2025.102264

Heinze, T. (2024). Multi-phase heat transfer in porous and fractured rock. *Earth-Science Reviews*, *251*, 104730. https://doi.org/10.1016/j.earscirev.2024.104730

Hoffmann, R., Dassargues, A., Goderniaux, P., & Hermans, T. (2019). Heterogeneity and prior uncertainty investigation using a joint heat and solute tracer experiment in alluvial sediments. *Frontiers in Earth Science*, *7*, 7–2019. https://doi.org/10.3389/feart.2019.00108

Irvine, D. J., Cranswick, R. H., Simmons, C. T., Shanafield, M. A., & Lautz, L. K. (2015). The effect of streambed heterogeneity on groundwater-surface water exchange fluxes inferred from temperature time series. *Water Resources Research*, *51*(1), 198–212. https://doi.org/10.1002/2014WR015769

Kaviany, M. (1995). *Principles of heat transfer in porous media* (2nd ed.). Springer. https://doi.org/10.1007/978-1-4612-4254-3

Lee, H. (2025). haegyeonglee/grainscale_ltne: Grainscale_ltne v1.0.0 (v1.0.0) [Software]. *Zenodo*. https://doi.org/10.5281/zenodo.17330106

Lee, H., Gossler, M., Zosseder, K., Blum, P., Bayer, P., & Rau, G. C. (2025). Laboratory heat transport experiments reveal grain-size- and flow-velocity-dependent local thermal non-equilibrium effects. *Hydrology and Earth System Sciences*, *29*(5), 1359–1378. https://doi.org/10.5194/hess-29-1359-2025

Levec, J., & Carbonell, R. G. (1985a). Longitudinal and lateral thermal dispersion in packed beds. Part ii: Comparison between theory and experiment. *AIChE Journal*, *31*(4), 591–602. https://doi.org/10.1002/aic.690310409

Levec, J., & Carbonell, R. G. (1985b). Longitudinal and lateral thermal dispersion in packed beds. Part I: Theory. *AIChE Journal*, *31*(4), 581–590. https://doi.org/10.1002/aic.690310408

Nield, D. A., & Bejan, A. (2017). *Convection in porous media* (5th ed.). Springer International Publishing.

Park, B.-H., & Lee, K.-K. (2021). Evaluating anisotropy ratio of thermal dispersivity affecting geometry of plumes generated by aquifer thermal use. *Journal of Hydrology*, *602*, 126740. https://doi.org/10.1016/j.jhydrol.2021.126740

Pophillat, W., Bayer, P., Teyssier, E., Blum, P., & Attard, G. (2020). Impact of groundwater heat pump systems on subsurface temperature under variable advection, conduction and dispersion. *Geothermics*, *83*, 101721. https://doi.org/10.1016/j.geothermics.2019.101721

Rau, G. C., Andersen, M. S., & Acworth, R. I. (2012). Experimental investigation of the thermal time-series method for surface water-groundwater interactions. *Water Resources Research*, *48*(3). https://doi.org/10.1029/2011WR011560

Rau, G. C., Andersen, M. S., McCallum, A. M., Roshan, H., & Acworth, R. I. (2014). Heat as a tracer to quantify water flow in near-surface sediments. *Earth-Science Reviews*, *129*, 40–58. https://doi.org/10.1016/j.earscirev.2013.10.015

Roshan, H., Cuthbert, M., Andersen, M., & Acworth, R. (2014). Local thermal non-equilibrium in sediments: Implications for temperature dynamics and the use of heat as a tracer. *Advances in Water Resources*, *73*, 176–184. https://doi.org/10.1016/j.advwatres.2014.08.002

Schornberg, C., Schmidt, C., Kalbus, E., & Fleckenstein, J. H. (2010). Simulating the effects of geologic heterogeneity and transient boundary conditions on streambed temperatures—Implications for temperature-based water flux calculations. *Advances in Water Resources*, *33*(11), 1309–1319. https://doi.org/10.1016/j.advwatres.2010.04.007

Shi, W., Wang, Q., Klepikova, M., & Zhan, H. (2024). New criteria to estimate local thermal nonequilibrium conditions for heat transport in porous aquifers. *Water Resources Research*, *60*(7), e2024WR037382. https://doi.org/10.1029/2024WR037382

Wagner, W., & Pruß, A. (2002). The IAPWS formulation 1995 for the thermodynamic properties of ordinary water substance for general and scientific use. *Journal of Physical and Chemical Reference Data*, *31*(2), 387–535. https://doi.org/10.1063/1.1461829

Wakao, N., & Kaguei, S. (1982). *Heat and mass transfer in packed beds*. Gordon and Breach Science Publishers.

Wakao, N., Kaguei, S., & Funazkri, T. (1979). Effect of fluid dispersion coefficients on particle-to-fluid heat transfer coefficients in packed beds: Correlation of Nusselt numbers. *Chemical Engineering Science*, *34*(3), 325–336. https://doi.org/10.1016/0009-2509(79)85064-2

Wang, C., & Fox, P. J. (2022). Numerical model for heat transfer in layered soil with local thermal nonequilibrium. *Journal of Geotechnical and Geoenvironmental Engineering*, *148*(4), 04022005. https://doi.org/10.1061/(ASCE)GT.1943-5606.0002760

Wang, C., & Fox, P. J. (2023). Validity of local thermal equilibrium assumption for heat transfer in a saturated soil layer. *Journal of Geotechnical and Geoenvironmental Engineering*, *149*(5), 06023002. https://doi.org/10.1061/JGGEFK.GTENG-11152

Wilkins, A., Green, C. P., & Ennis-King, J. (2021). An open-source multiphysics simulation code for coupled problems in porous media. *Computers & Geosciences*, *154*, 104820. https://doi.org/10.1016/j.cageo.2021.104820

Zhu, L.-T., Liu, Y.-X., & Luo, Z.-H. (2019). An enhanced correlation for gas-particle heat and mass transfer in packed and fluidized bed reactors. *Chemical Engineering Journal*, *374*, 531–544. https://doi.org/10.1016/j.cej.2019.05.194